



HAL
open science

Drastic Change in Zinc Speciation during Anaerobic Digestion and Composting: Instability of Nanosized Zinc Sulfide

Maureen Le Bars, Samuel Legros, Clément Levard, Perrine Chaurand, Marie Tella, Mauro Rovezzi, Patrick Browne, Jérôme Rose, Emmanuel Doelsch

► **To cite this version:**

Maureen Le Bars, Samuel Legros, Clément Levard, Perrine Chaurand, Marie Tella, et al.. Drastic Change in Zinc Speciation during Anaerobic Digestion and Composting: Instability of Nanosized Zinc Sulfide. *Environmental Science and Technology*, 2018, 52 (22), pp.12987-12996. 10.1021/acs.est.8b02697 . hal-01919881

HAL Id: hal-01919881

<https://hal.science/hal-01919881v1>

Submitted on 14 Mar 2019

HAL is a multi-disciplinary open access archive for the deposit and dissemination of scientific research documents, whether they are published or not. The documents may come from teaching and research institutions in France or abroad, or from public or private research centers.

L'archive ouverte pluridisciplinaire **HAL**, est destinée au dépôt et à la diffusion de documents scientifiques de niveau recherche, publiés ou non, émanant des établissements d'enseignement et de recherche français ou étrangers, des laboratoires publics ou privés.

16

17 KEYWORDS. Digestate, Compost, X-ray absorption spectroscopy (EXAFS), Organic waste,
18 Agricultural recycling, Nanoparticles

19

20 ABSTRACT. Zinc (Zn) is a potentially toxic trace element that is present in large amounts in organic
21 wastes (OWs) spread on agricultural lands as fertilizer. Zn speciation in OW is a crucial parameter to
22 understand its fate in soil after spreading and to assess the risk associated with agricultural recycling of
23 OW. Here, we investigated changes in Zn speciation from raw OWs up to digestates and/or composts for
24 a large series of organic wastes sampled in full-scale plants. Using extended X-ray absorption fine
25 structure (EXAFS), we show that nano-sized Zn sulfide (nano-ZnS) is a major Zn species in raw liquid
26 OWs and a minor species in raw solid OWs. Whatever the characteristics of the raw OW, anaerobic
27 digestion always favors the formation of nano-ZnS (>70% of zinc in digestates). However, after 1 to 3
28 months of composting of OWs, nano-ZnS becomes a minor species (<10% of zinc). In composts, Zn is
29 mostly present as amorphous Zn phosphate and Zn sorbed to ferrihydrite. These results highlight (i) the
30 influence of OW treatment on Zn speciation and (ii) the chemical instability of nano-ZnS formed in OW
31 in anaerobic conditions.

32 **Introduction**

33 Organic waste (OW) production is steadily increasing as a result of the growth of the world
34 population¹ and there is thus an urgent need for sustainable OW management. OWs have different
35 origins: agricultural (livestock slurries, harvest residues), urban (sewage sludge), industrial (food
36 industry by-products) and municipal waste (OW collected from private households).² Among the

37 solutions for sustainable OW management, anaerobic digestion (AD) is gaining interest because biogas
38 can be produced by biological decomposition of organic matter² and because of the value of the organic
39 residue (called digestate) as fertilizer.³ The short term advantages of applying digestate on cropped soils
40 have already been evidenced,⁴ but recently, questions have been raised about the long-term impact of the
41 accumulation of trace elements (TEs) in soils after recycling of digestate.⁵ With increasing interest in
42 anaerobic digestion (AD) worldwide, it is crucial to determine the risk associated with agricultural
43 recycling of digestate.

44 Among all the TEs present in OWs, zinc (Zn) is the most applied on agricultural lands.^{6,7} In particular,
45 sewage sludge and livestock manures used as amendments have relatively high concentrations of Zn
46 (321-4753 mg/kg).⁸⁻¹¹ As Zn has been shown to be hazardous for plants,¹²⁻¹⁵ regulations have been
47 introduced to limit the environmental impact of OW recycling. However, the regulations are based on
48 total Zn (and more generally on TE) concentrations in OW,^{16,17} whereas Zn eco-toxicity not only
49 depends on the total concentration but also on Zn speciation, which determines its bioavailability.¹⁸ For
50 instance, different toxicity mechanisms have been described when *Escherichia coli* were exposed to
51 nanoparticulate ZnO or dissolved Zn.¹⁹

52 Recent studies using X-ray absorption spectroscopy (XAS) have shown that part of Zn is present as
53 zinc sulfide (ZnS) in raw OWs^{20,21} and digestates.^{20,22-26} This technique is thus suitable to determine Zn
54 speciation in a complex matrix such as OW.^{27,28} Surprisingly, the proportion of ZnS present in OWs is
55 wide, ranging from 0 to 100% in raw OWs^{20,21} and 0 to 96% in digestates.^{20,22-25} These differences can
56 be explained by several factors including (i) the type of reactor sampled (lab-scale vs. full-scale
57 reactors), (ii) the origin and the nature of the OW (agricultural vs. urban, solid vs. liquid) and/or (iii) the
58 processing steps that may differ from one laboratory/site to another (e.g. hydraulic retention time,
59 storage conditions). All these parameters can affect the physical-chemical conditions of the systems,
60 which, in turn, control the speciation of Zn present in raw or digested OWs.

61 Some studies have reported that Zn K-edge extended X-ray absorption fine structure (EXAFS) spectra
62 in OWs are (i) less structured than for a crystalline ZnS, and (ii) are similar to what is observed for 3-4
63 nm ZnS nanoparticles (referred to hereafter as nano-ZnS).^{20,21,26} The presence of nano-sized and not
64 well-organized ZnS in OW is thus suspected. This result is important when assessing the agro-
65 environmental risks of agricultural recycling of OWs. Indeed, although nano-ZnS eco-toxicity has been
66 poorly studied, nanoparticles are generally known for their increased reactivity and associated toxic
67 effects in comparison with their bulk analogs.²⁹

68 As the increased reactivity of nanoparticles favors their dissolution and transformation,²⁹ the chemical
69 stability of nano-ZnS during treatment needs to be assessed. Recently, it was shown that ZnS present in
70 sewage sludge digestates was partly or totally oxidized during composting²²⁻²⁵ suggesting low stability of
71 ZnS formed during AD. Moreover, no available information is available on Zn speciation in the
72 intermediate products (solid/liquid fractions of digestates) even though these may also be spread on soils.

73 We conducted a systematic study to investigate the speciation of Zn in raw OWs and treated OWs in a
74 wide range of full-scale OW treatment plants chosen to represent the most common origins of OW
75 (agricultural, urban, industrial OW) and treatment processes (AD, composting). Special care was taken
76 to sample OWs throughout the process to assess changes in Zn speciation during treatment. Nine full-
77 scale treatment plants that process agricultural, urban and industrial OW were sampled and X-ray
78 absorption spectroscopy was used to investigate the speciation of Zn in raw and treated OWs.

79 **Experimental section**

80 **Preparation of organic waste samples**

81 Organic wastes were sampled in nine different full-scale treatment plants distributed throughout
82 France. The plants were chosen to represent the most common types of raw OW used as feedstock for
83 anaerobic digestion (AD) and composting: agricultural waste (livestock effluents, crop residues, etc.),

84 urban wastes (sewage sludge, catering and major-food retailer wastes) and industrial wastes (from the
85 food industry). For the sake of clarity, the treatment plants are separated into three groups based on the
86 origin of the raw OW used as feedstock: Urban (sewage sludge), Agri (agricultural waste), Central (mix
87 of different types of OW digested in a centralized plant). Depending on the plant, OWs are treated by
88 AD and/or composting. Some of the AD plants apply a post-treatment to the digestate: solid/liquid
89 separation, pellet making and/or composting. For example, the Urban 2 plant includes a pelletizing unit
90 (drying, liming and pressing into pellets) to process the solid digestate. For AD, three types of reactors
91 are used depending on the dry matter (DM) content: wet reactors (DM < 16%), semi-dry reactors
92 (DM=[16-22%]) and dry reactors (DM=[22-40%]).³⁰ All digested OW were processed in wet reactors
93 except Agri 2 (digestate DM content 19%). Another specificity of this plant the temperature (45°C) used
94 is higher than the mesophilic temperature (32-42°C) used in all the other digesters. The characteristics of
95 the OW treatment plants are listed in Table 1.

		Anaerobic digestion			Composting	
Site	Composition of raw organic wastes	Reactor Size (m ³)	Duration (days)	Solid/liquid separation characteristics	Duration (weeks)	Co-substrate
Urban-1	Sewage sludge	6200	29	Filter press – 19m ³ /h	4	Green waste
Urban-2	Sewage sludge	6000	34	Centrifugation – 20 m ³ /h	12	Green waste
Urban-3	Activated and centrifuged sewage sludge	-	-	-	6	Green waste
Agri-1	Pig slurry + co-substrates ¹	950	38	Centrifugation – 8m ³ /h Solid digestate stockpiled	12	None
Agri-2	Solid cow manure + co-substrates ²	740	42	-	-	-
Agri-3	Solid cow manure	-	-	-	n/a	None
Central-1	Livestock effluents ³ + sewage sludge + food industry waste + harvest residues	1600	70	Screw press – n/a Solid digestate stockpiled	-	-
Central-2	Pig slurries + food industry waste + harvest residues + poultry manure	6000	30	Centrifugation – 8 m ³ /h	-	-
Central-3	Catering and waste from major food retailers + cow slurries + food industry waste + wine making waste	8000	90	-	-	-

96 Table 1: Description of the treatment plants

97 ¹harvest residues, grass clippings

98 ²harvest residues, fecal matter from cattle intestines, grass clippings, poultry litter

99 ³ solid cow, sheep and horse manure - cow and pig slurries

100 At each full-scale plant, around 3 kg of dry matter of OWs were sampled at different steps of
101 the treatment. At the seven AD plants (Urban 1-2, Agri 1-2 and Central 1-2-3), OW was sampled
102 just before AD (samples called “raw OW”) and just after AD (samples called “digestate”). When
103 a digestate post-treatment was included in the process, the intermediate products and the final
104 products (ready to apply as fertilizer) were sampled (solid/liquid fractions of digestate called
105 “solid digestate” and “liquid digestate” respectively, pellets and compost). At the two
106 composting plants (Agri-3, Urban-3), raw OW was sampled before composting, and compost
107 was sampled. All the samples were frozen at -20 °C, at the latest three days after on-site
108 sampling.

109 **Physical-chemical analyses**

110 Dry matter (DM) content of the OW samples was determined at 60 °C by weight (+/- 0.2%).
111 pH was measured directly in liquid OW samples. The pH of solid OW samples was measured
112 after water extraction (ratio of OW to water volume 1:5) according to the ISO 10390 standard.
113 Each pH value is given with an uncertainty of +/- 0.1. Oxidation-reduction potential (ORP) was
114 measured in liquid samples only using a platinum wire electrode (Hamilton Polilyte Plus ORP
115 Arc 120) with +/- 20 mV uncertainty. OW samples were freeze-dried, ground and homogenized
116 for digestion using a mixture of HF, HNO₃ and HClO₄ (ISO 14869-1). Next, concentrations of
117 trace elements were determined using an inductively coupled plasma mass spectrometer (ICP-
118 MS iCAP™ Q Thermo Scientific). Before each element was analyzed, the method of
119 quantification was checked using certified reference material (sewage sludge (BSR 146R) and
120 soil (LAOM CRM 7004)). Measurement uncertainty was less than 15%. Total carbon (ISO
121 10694) was determined by dry combustion (Dumas) with an elemental NC 2100 Soil Analyzer
122 (Thermo Electron Corp.) The method of analysis was validated using certified reference material
123 (Orchard Leaves Standard 502-055). Uncertainty was less than 5%. Inorganic carbon (ISO

124 10693) was determined (uncertainty +/-2%) with a Bernard Calcimeter by adding HCl and
125 measuring released CO₂. Organic carbon (Corg) was deduced from the difference between total
126 and inorganic carbon. Uncertainty of Corg concentration (+/- 7%) was determined by adding
127 absolute uncertainties of total C and inorganic C. One replicate was performed for each OW and
128 each parameter.

129 **Preparation of samples and reference compounds for EXAFS analysis**

130 When fresh and freeze-dried OW samples were compared using Zn K-edge EXAFS spectra, no
131 influence of the freeze-drying process was observed (Figure S1). Therefore, all OW samples
132 were freeze-dried before EXAFS analysis. Potential changes in Zn speciation during the aging of
133 freeze-dried samples were also assessed. No change in Zn speciation was observed after three
134 weeks of aging at room temperature (Figure S2). However, after six months and one year of
135 aging of the freeze-dried sample, Zn speciation in OW was altered. To avoid these changes, all
136 freeze-dried samples were stored at -20 °C until EXAFS analysis. Indeed, at -20 °C, there was no
137 change in Zn speciation after 6 months of aging (Figure S3). Freeze-dried OW samples were
138 cryo-ground before analysis (Retsch MM400).

139 Nano-ZnS reference compound was synthesized by mixing sodium sulfide (Na₂S) and zinc
140 chloride (ZnCl₂) solutions at a molar ratio S/Zn of 1 to obtain a final ZnS concentration of 4 g/L.
141 After eight days of agitation, the suspension was dialyzed (MWCO 1kDa) using ultrapure water
142 for two days to remove excess Na⁺ and Cl⁻ ions. The final nano-ZnS suspension was freeze-dried
143 and the resulting solid was analyzed by X-ray diffraction (X'Pert Pro MPD, Panalytical). A
144 crystallite size of 3 +/- 0.4 nm was determined using the Scherrer equation³¹ (Figure S4). A
145 commercial ZnS with a crystallite size of 20 nm (Figure S4) was purchased from Sigma Aldrich.
146 Amorphous zinc phosphate (Am-Zn-phosphate) was synthesized following the protocol of Bach
147 et al.³² Briefly, NaHPO₄⁻ (0.010 M, pH adjusted to 11.9) and ZnCl₂ (0.015 M) solutions were

148 mixed and immediately centrifuged at 12,544 g for 5 min and rinsed three times with acetone (>
149 99%, VWR). The resulting solid was dried under vacuum. The X-ray diffraction (Figure S5)
150 pattern is in accordance with the result obtained by Bach et al. (2015).³² Reference compounds
151 were diluted in polyvinylpyrrolidone powder, ground and pressed into pellets for EXAFS
152 analysis.

153 **EXAFS spectra acquisition and analysis**

154 Zn K-edge X-ray absorption spectra were recorded at the SSRL (Stanford, USA) on the 11-2
155 beamline and at the ESRF (Grenoble, France) on the BM30B (FAME) beamline. Each spectrum
156 was measured at liquid helium temperature to prevent the beam damaging the samples. On both
157 beamlines, the spectra of the OW samples were measured in fluorescence mode with a 30-
158 element solid state Ge detector. The spectra of the reference samples were measured in
159 transmission mode. One spectrum is the average of two to nine scans, depending on the
160 concentration of Zn and the noise level. Each scan was measured on a different spot on the pellet
161 to limit beam damage. Energy calibration was performed using metallic Zn reference foil
162 (absorption edge defined at 9659 eV). Normalization and data reduction were performed
163 according to standard methods³³ using Athena software.³⁴

164 A library of Zn reference compound spectra was used to identify Zn species in the OW. Least
165 square linear combination fitting (LCF) was performed for each OW spectrum over a k-range of
166 2.5 - 10.6 Å⁻¹ using Athena software.³⁴ The library of Zn reference compounds consisted in
167 nano-ZnS, Am-Zn-phosphate, commercial ZnS (see previous section) and reference compounds
168 described elsewhere^{20,35-39} (Zn-cysteine, Zn-histidine, Zn-malate, Zn-sorbed to ferrihydrite (Zn-
169 FeOx), Zn-methionine, Zn-cryptomelane Zn-phosphate, Zn-phytate, Zn-Goethite, Zn-oxalate-
170 hydrate, Sphalerite, Smithsonite, Zincite, Zn hydroxide (Figure S6)). Residual factor of LCF was

171 calculated as follows: $R = \Sigma(k^3\chi(k)_{exp} - k^3\chi(k)_{fit})^2 / \Sigma(k^3\chi(k)_{exp})^2$. At each step of the
172 fitting, an additional reference spectrum was added if the two following conditions were true: the
173 R factor decreased by 20% or more and the additional reference had a contribution equal to or
174 higher than 10% among Zn-species. The uncertainty of this LCF method was estimated at +/-
175 15%.³³

176 **Results and Discussion**

177 **Changes in physical-chemical characteristics of OWs during treatment**

178 The physical-chemical characteristics of OWs during treatment were identified as these
179 parameters can control the speciation of Zn.

180 Table 2: Characteristics of raw and treated OWs (DM= dry matter, ORP=oxidation reduction
181 potential, Corg=organic carbon). The concentrations of all the elements are expressed on a dry
182 matter (DM) basis. Values are given +/- 15% for [Zn], [P] and [Fe], +/- 7% for [Corg], +/- 20
183 mV for ORP, +/- 0.1 for pH and +/- 0.2% for DM)

Treatment plant	Sample	DM %	pH	[Zn] mg/kg	[Fe] g/ kg	[P] g/ kg	[Corg] %	ORP (mV)
Urban-1	Raw OW	3.4	6.3	701	49.28	33.80	40	-213
	Digestate	3.1	7.3	822	56.73	39.21	34	-248
	Solid digestate	18.7	6.6	807	87.80	38.92	32	
	Solid digestate + green waste	41.4	6.9	275	25.56	11.00	43	
	Compost	58.2	7.0	423	37.77	17.54	30	
Urban-2	Raw OW	5.3	5.2	475	30.63	20.74	50	-138
	Digestate	2.7	7.6	694	48.61	43.01	37	-249
	Solid digestate	16.4	6.8	696	52.20	40.01	37	
	Pellets	91.7	12.2	543	41.48	33.43	29	
	Compost	96.6	7.75	711	62.04	31.58	27	
Urban-3	Raw OW	17.8	5.9	566	5.23	27.39	49	
	Compost	65.1	7.0	452	10.64	21.42	26	
Agri-1	Raw OW	5.1	6.4	398	2.11	13.72	48	-187
	Digestate	2.5	7.9	723	3.13	16.27	35	-233
	Liquid digestate	2.9	8.1	1 241	4.40	17.48	36	-262
	Solid digestate	36.8	6.8	547	5.34	34.51	34	
	Compost	59.7	6.8	697	8.96	42.27	22	
Agri-2	Raw OW	37.3	8.8	70	0.42	5.27	46	
	Digestate	19.0	9.1	244	3.74	12.32	38	
Agri-3	Raw OW	23.0	9.2	83	1.27	4.79	43	
	Compost	38.9	9.3	116	1.65	5.14	42	
Central-1	Raw OW	8.0	5.7	325	18.13	13.13	42	-177
	Digestate	11.0	7.9	701	40.61	21.22	32	-241
	Liquid digestate	5.8	7.8	663	38.02	19.71	31	-255

	Solid digestate	26.5	7.6	178	14.19	8.60	47	
	Raw OW	14.7	6.3	533	18.10	16.45	57	-209
Central-2	Digestate	7.4	8.5	841	27.89	32.07	40	-347
	Solid digestate	23.5	6.2	995	32.96	27.43	41	
	Raw OW	28.0	4.7	64	2.79	5.62	37	-112
Central-3	Digestate	7.4	7.9	201	9.05	14.36	34	-341

184 *Dry Matter, organic carbon and pH*

185 The range of dry matter (DM) content in the raw OWs used in this study was wide (ranging
186 from 3 to 37%, Table 2), reflecting the diversity of raw OWs used in the full-scale treatment
187 plants. Corg and DM content in the digestate were lower than in raw OW, due to the organic
188 matter released as biogas during AD: 9 to 30% of initial Corg in the raw OW is converted into
189 CH₄ and CO₂ (main gas phases of biogas),² which is in agreement with previous results.²⁰ Urban-
190 1 and Central-1 are exceptions to this trend, possibly be explained by the heterogeneity of OW
191 samples over time.⁴⁰ Similarly, Corg content decreased during composting: 3 to 47% of initial
192 Corg (in raw OW for Urban-3, Agri-3, solid digestate for Urban-1, Agri-1 or pellets for Urban-2)
193 was converted into CO₂ by carbon mineralization. Despite this C loss, DM content increased
194 after composting due to greater water loss during the aerobic process. pH values ranged from 4.7
195 to 9.2 in raw OWs and increased after AD due to the degradation of volatile fatty acids, as
196 observed in many studies.^{8,9,41-43}

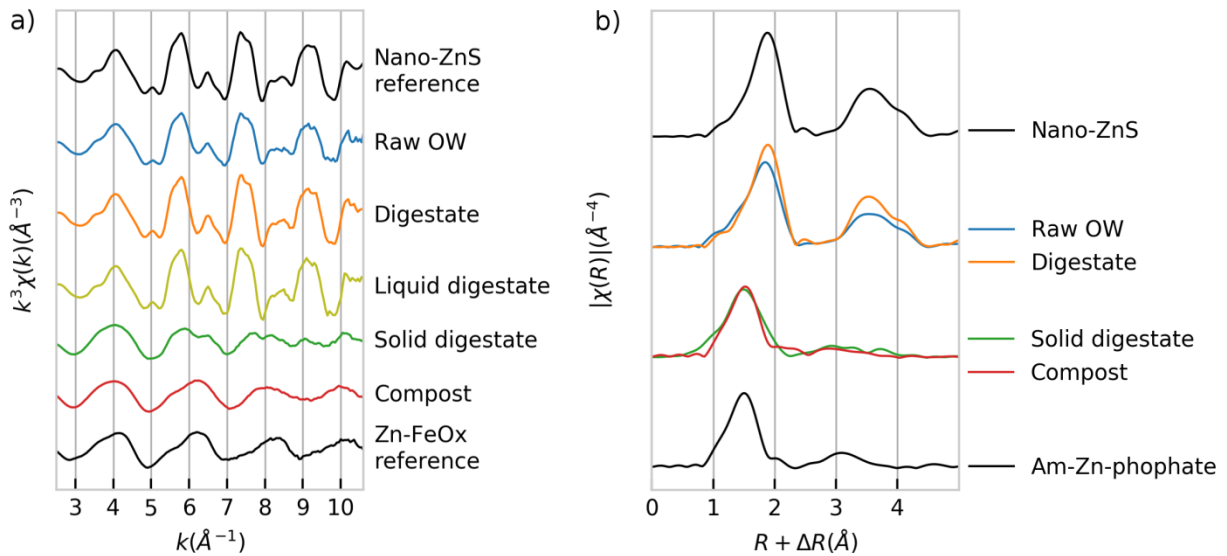
197 *Zn concentration*

198 The concentration of Zn (Table 2) in raw OWs ranged from 64 to 701 mg/kg. This wide range
199 can be explained by the different origins of the raw OW. Sewage sludges (raw OW in Urban-1, -
200 2, -3) tended to have high concentrations of Zn (475 – 701 mg/kg) as described earlier.⁹⁻¹¹ In

201 agricultural wastes (Agri-1, -2, -3), we observed high variability of Zn concentrations among
202 treatment plants. The Zn concentration in raw OW sampled from Agri-1 was relatively high (398
203 mg/kg) whereas it was lower in samples from Agri-2 and Agri-3 (70 and 83 mg/kg,
204 respectively). Raw OW from Agri-1 contained 80% of pig slurry whereas raw OWs from Agri-2
205 and Agri-3 contained solid cow manure. The Zn concentration in pig slurries is always
206 significantly higher than in cattle slurries^{8,44} because of the addition of Zn in pig feed and low
207 intake by the animal.⁴⁵ In samples from the centralized AD plants (Central-1, -2, -3), we also
208 observed a wide range of Zn concentrations among sites. Raw OWs with high Zn concentration
209 were those that partly comprised pig slurries (Central-1: 325 mg/kg) and/or sewage sludge
210 (Central-2: 533 mg/kg) in contrast to Central-3 (64 mg/kg) that contained neither. These results
211 show that the concentration of Zn in raw OWs is driven by the origin of the OW.

212 Similar changes in Zn concentrations during OW treatments (AD or composting) were
213 observed whatever the plant considered. Zn is conserved during AD while organic matter is lost.
214 Therefore Zn concentration in digestates was higher than in raw OW, confirming previous
215 observations.^{9,20,42} Likewise, Zn concentrations increased following composting as reported by
216 Knoop et al.⁴² The only exception was Urban-3 compost where the decrease in Zn concentration
217 could be due to dilution caused by the addition of green waste.

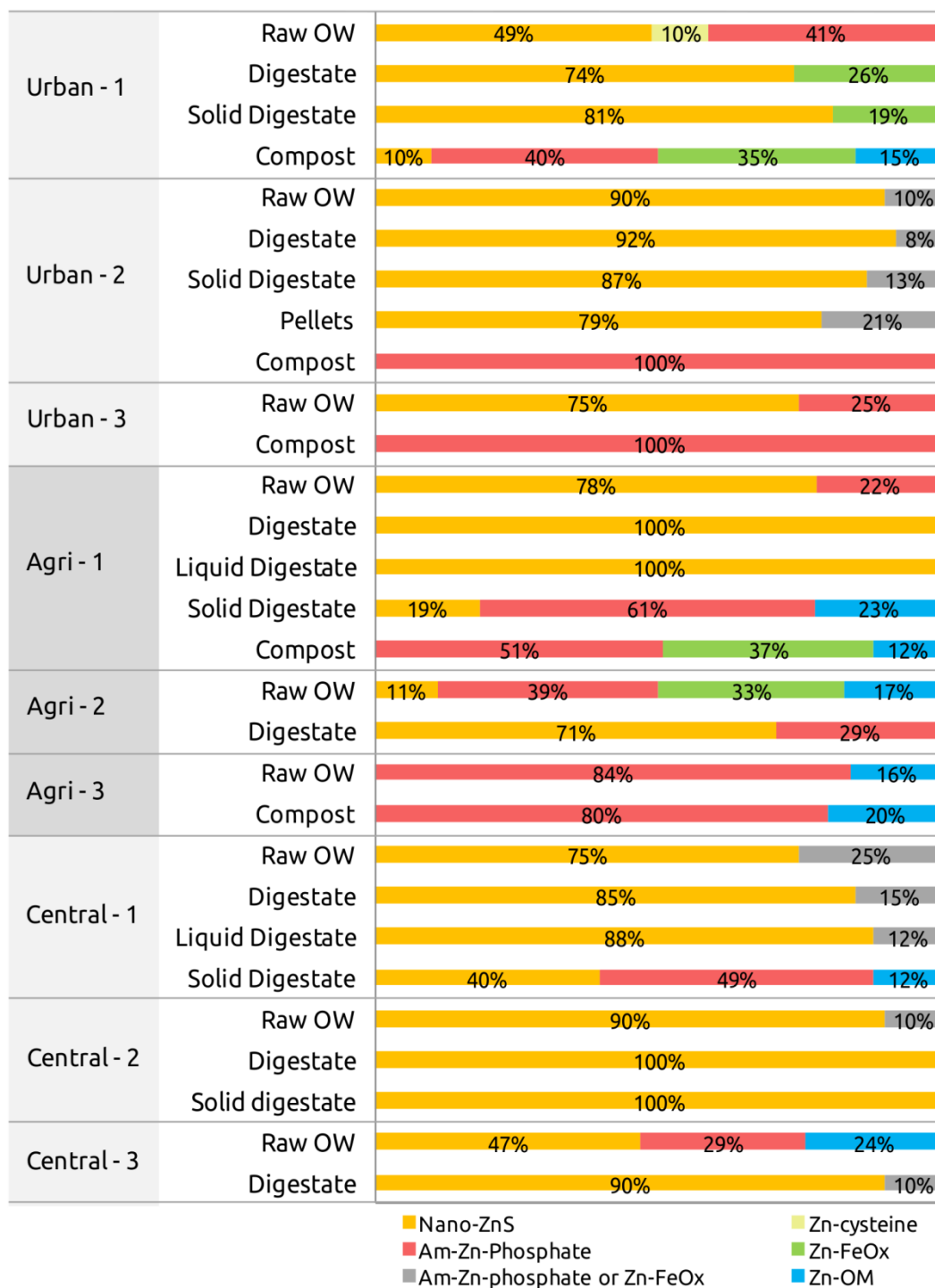
218 **Change in Zn speciation during treatment**



219
 220 Figure 1: (a) Zn K-edge extended X-ray absorption fine-structure spectroscopy (EXAFS) spectra
 221 and (b) respective Fourier transforms (FT) of raw and treated OWs at different steps of the
 222 treatment at the Agri-1 site. Nano-ZnS and Zn-FeOx reference compounds have been added for
 223 EXAFS comparison.

224 First, a visual comparison of EXAFS spectra and the corresponding Fourier transforms (FT) of
 225 the samples at different steps of the treatment already provides qualitative insight into the change
 226 in Zn speciation during the process. Zn K-edge EXAFS spectra (Figure 1 (a)) are characteristic
 227 of Zn atomic environment (number of neighboring atoms, their distance from absorbing Zn
 228 atom, static disorder). Fourier transform of EXAFS spectra (Figure 1 (b)) gives an atomic radial
 229 distribution function for which the peak position is specific to an interatomic distance (from a Zn
 230 atom) and peak intensity depends on the number of neighboring atoms and static disorder. As an
 231 example, Figure 1 shows spectra and the corresponding FT obtained at the Agri-1 plant. Data for
 232 the eight other plants are presented in supplementary information SI-4.

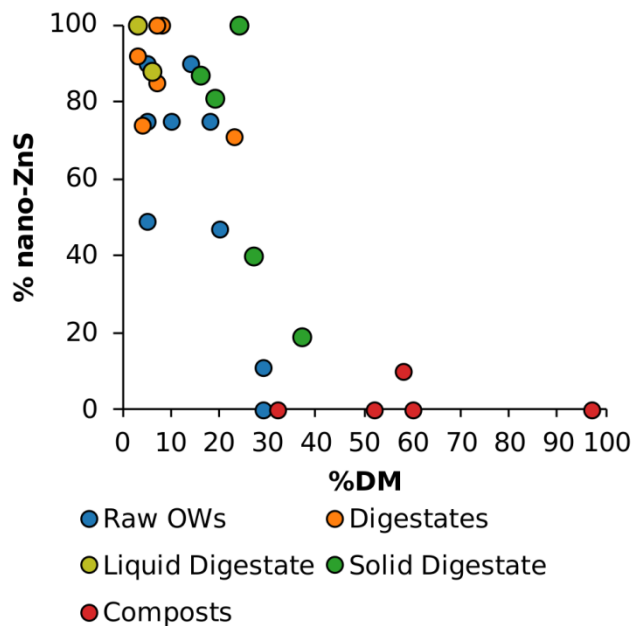
233 EXAFS spectra of raw OW and digestate from Agri-1 strongly resembled the spectrum of the
234 nano-ZnS reference compound (Figure 1 (a)). Centrifugation of Agri-1 digestate resulted in two
235 fractions with contrasted Zn speciation. The EXAFS spectrum of the liquid digestate was very
236 similar to the spectrum of the nano-ZnS reference compound whereas the solid fraction of the
237 digestate tended to be closer to the spectrum of the Zn-FeOx reference compound. The FT can be
238 used to distinguish the shift from a Zn—S contribution for raw OW, digestate and liquid
239 digestate to a Zn—O contribution for solid digestate and compost. In addition to this visual
240 inspection of the spectra, linear combination fitting (LCF) was performed to obtain quantitative
241 results on Zn speciation in OWs in all the samples. The modeled spectra of all the samples were
242 compared to experimental spectra (Figure S7). The quantitative LCF results (expressed as a
243 percentage of each Zn species) obtained for samples from the nine treatment plants are shown in
244 Figure 2. Experimental data were modeled with 1 to 4 references and total contributions ranging
245 from 91 to 107%. The contributions of Zn species were normalized to 100% for easier
246 comparison. R-factor of the LCFs ranged from 0.0057 to 0.0292. For the sake of clarity,
247 reference compounds for Zn bound to organic matter (Zn-malate, Zn-histidine or Zn-methionine,
248 see Table S1 and Figure S6) are represented as “Zn-OM”. Also, in some cases, when the
249 contributions of amorphous Zn phosphate (Am-Zn-Phosphate) and Zn bound to ferrihydrite (Zn-
250 FeOx) were less than 25%, it was impossible to differentiate between them (Figure S8). In this
251 particular case, they are represented as “Am-Zn-phosphate or Zn-FeOx”.



252

253 Figure 2: Zn speciation determined from the linear combination fitting of the Zn K-edge

254 extended X-ray absorption fine-structure spectroscopy data for all raw and treated OWs.



256

257 Figure 3: Percentage of nano-ZnS determined by linear combination fitting of the Zn K-edge
 258 extended X-ray absorption fine-structure spectroscopy data as a function of dry matter (DM)
 259 content for all raw and treated OWs (except for the pellets from Urban-2 as the treatment
 260 consisting of drying, liming and pressing is specific).

261 *Zn speciation in raw OWs*

262 Nano-ZnS was found to be the main Zn species in raw OWs (ranging from 47 to 90%) except
 263 in samples from Agri-2 (11%) and Agri-3 (no detection). The relatively wide range of nano-ZnS
 264 may be due to the nature of OW and more importantly to their different physical-chemical
 265 storage conditions (DM content and ORP). Indeed, Figure 3 reveals an opposite trend between
 266 the percentage of nano-ZnS in raw OW and their DM content. Interestingly, samples from Agri-2
 267 and Agri-3, which did not contain significant amounts of nano-ZnS, had the highest DM content
 268 of all the raw OW samples (37 and 23% DM, respectively) (Figure 3). We were unable to
 269 measure an ORP value for these samples. However, it is probable that storage at such high DM

270 content favors aerobic conditions. Conversely, reducing conditions in raw liquid OWs from
271 Urban-1,2,3, Agri-1, and Central-1,2 were favored, as shown by ORP values (-213 to -138 mV).
272 This could enhance sulfur reduction and hence the formation of nano-ZnS with the presence of
273 sulfate reducing bacteria (SRB).⁴⁶⁻⁴⁸ The second main Zn species in raw OWs was amorphous
274 Zinc phosphate (Am-Zn-phosphate) which accounted for 22 to 84% of Zn species. This is in
275 agreement with the high affinity of Zn for phosphate compounds.⁴⁹ Hopeite (crystalline zinc-
276 phosphate) has already been evidenced in previous studies as a major Zn phase in OW.^{20,23,24}

277 *Zn speciation in digestates*

278 Whatever the raw OW, nano-ZnS was the dominant Zn species in the digestates. The
279 contribution of nano-ZnS ranged from 71 to 100% in the digestates (Figure 2). What is more, the
280 proportion of nano-ZnS always increased after AD (except in samples from Urban-2) (Figure 2).
281 The more reducing conditions in the digestate compared with in raw OWs, as illustrated by ORP
282 values (from -213 to -112mV in raw OWs and from -347 to -233 mV in digestates, see Table 2),
283 may favor the formation of zinc sulfide. Indeed, AD conditions favor the presence of sulfate
284 reducing bacteria (SRB), which convert sulfate to sulfide.⁵⁰

285 *Zn speciation in the liquid and solid fractions of the digestate*

286 Zn speciation in the liquid and solid fractions of digestate was influenced by the storage
287 conditions. The speciation of Zn in the solid fractions of digestate from Agri-1 and Central-1 had
288 low percentages of nano-ZnS and differed from that of the digestates, whereas nano-ZnS were
289 still present in samples from Urban-1, Urban-2 and Central-2. Such differences can be explained
290 by the different sampling conditions. Agri-1 and Central-1 solid digestates were sampled in the
291 storage pile whereas the other solid fractions of digestates were sampled directly at the end of the

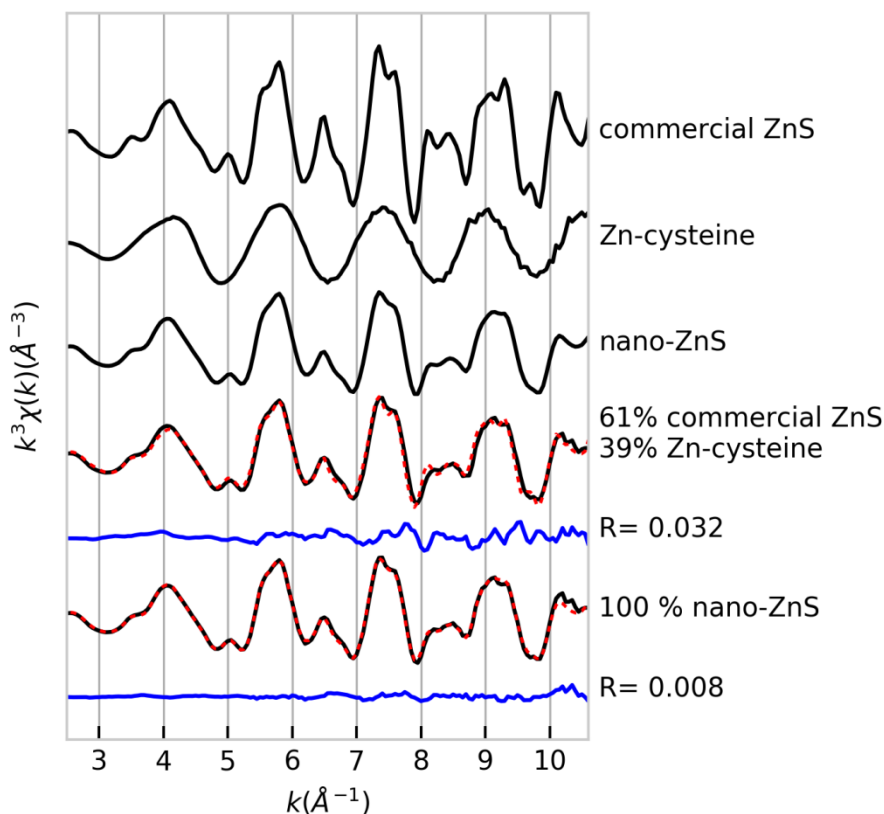
292 separation process. When sampled in the storage pile, OWs had been exposed to the atmosphere
293 for some days so nano-ZnS may have been oxidized. Nano-ZnS was detected in the liquid
294 fraction after phase separation (Agri-1 and Central-1), which can be explained by the low DM
295 content of the liquid digestates (3 and 6%, respectively). In addition, the storage of liquid
296 digestate without mixing maintains anaerobic conditions, as shown by the ORP values (-262 and
297 -255mV, respectively). Nano-ZnS speciation was preserved after Urban-2 solid digestate was
298 pelleted, probably because the pellets were sampled immediately after processing and exposure
299 to the atmosphere was thus limited. These results highlight the reactivity of ZnS formed in OW
300 and the influence of OW storage and sampling conditions on Zn speciation.

301 *Zn speciation in composts*

302 In compost, Zn speciation differed dramatically from Zn speciation in digestates (Figure 2).
303 Nano-ZnS was no longer observed in any of the composts, (except in Urban-1 compost in which
304 10% of Zn remained in the form of sulfide). This means that nano-ZnS initially present in raw
305 OW and formed during AD disappeared after four to 12 weeks of composting (Table 1).
306 Previous studies on sewage sludge composted at laboratory scale^{24,25} and sewage sludge
307 composted at full scale²³ still revealed ZnS or Zn-cysteine (amino acid containing thiol side
308 chain) as a minor part of Zn speciation in compost (26 - 30% for ZnS and 6 -21%, for Zn-
309 cysteine). The main species of Zn in all the composts studied was Am-Zn-phosphate (from 40 to
310 100%). The second main species was Zn-FeOx present in composts from Urban-1 and Agri-1.
311 Zn associated with organic matter (OM) was present in three composts (Urban-, Agri-1 and
312 Agri-3) as a minor species (12 to 20% of Zn). Other studies on Zn speciation in compost of
313 sewage sludges have shown that the main Zn phase is Zn-FeOx (35-71%), followed by hopeite
314 (crystalline Zn-phosphate, 14-31%).²³⁻²⁵ There are therefore significant differences in results

315 obtained in previous work and the present study. These discrepancies can be explained by the
316 introduction of a new reference compound spectrum in the EXAFS library and LCF, the
317 amorphous Zn phosphate that matches the speciation of Zn in the composts we studied very well.
318 To our knowledge, this is the first evidence for the presence of amorphous zinc phosphate in
319 composted OWs. The presence of such amorphous compounds could be explained by the
320 inhibition of phosphate crystallization due to the presence of large amounts of organic matter in
321 the composts.

322 The nano-size of ZnS explains its ephemeral nature



323
324 Figure 4: Comparison of Zn K-edge extended X-ray absorption fine-structure spectroscopy
325 spectra of Agri-1 digestate, synthesized nano-ZnS and commercial ZnS.

326 EXAFS spectra of OW samples containing ZnS strongly resembled nano-ZnS reference
327 spectra. Figure 4 shows that oscillations at 5, 6.5, 8.5 and after 10\AA^{-1} are much less intense for
328 the Agri-1 digestate spectrum than for commercial ZnS. Visually, Agri-1 digestate spectrum is
329 very similar to the nano-ZnS spectrum and this similarity was observed in all OWs containing
330 ZnS (Figure S7). In addition, the nano-ZnS reference compound was always selected by LCF
331 calculation to model the experimental signal unlike the commercial ZnS compound, which was
332 never selected (Table S1 for detailed results of LCF). The EXAFS signal for nano-ZnS had
333 smaller oscillations than the commercial ZnS due to a smaller number of Zn atoms in the second
334 coordination shell. Indeed, the contribution of under-coordinated Zn atoms located at the surface
335 to the EXAFS signal increases with a decrease in particle size. Thus when we detected ZnS in
336 raw OWs and digestates, we suspected ZnS would be nano-sized.

337 As the EXAFS technique gives averaged information on Zn local environment, this nano-ZnS
338 EXAFS signature probably reflects the average distribution of ZnS of different sizes and
339 crystallinities that is equivalent, on average, to the 3 nm-nano-ZnS reference used in this study.
340 Indeed, the less intense EXAFS oscillations for the Agri-1 digestate compared to commercial
341 ZnS could be due to the presence of both crystalline ZnS (such as commercial ZnS) and Zn-
342 cysteine, which is less structured. This combination was tested by LCF to fit Agri-1 and
343 indicated a significantly higher residue (+300%) than the fit with nano-ZnS (Figure 4).

344 Legros et al.²⁰ also used a nano-ZnS reference spectrum to model OW spectra of lab-scale raw
345 OWs and digestates composed of pig slurry, sewage sludge and municipal wastes. Our results
346 extend the observation of a nano-ZnS signature in raw OWs and digestates from different origins
347 and for samples taken from full-scale plants. The previous imaging of nano-ZnS (2.5 to 7.5 nm)

348 in digested sewage sludge²⁶ reinforces the hypothesis of the presence of nano-ZnS in OW
349 samples.

350 Anaerobic digestion and anaerobic storage of OW create environmental conditions that are
351 favorable for nano-ZnS precipitation. For example, sulfate-reducing bacteria (SRB) can be
352 present in AD digesters because of anaerobic conditions and high sulfate concentration.⁵⁰ Nano-
353 ZnS has been observed in in-situ biofilms containing a majority of SRB.^{46,51} The presence of
354 SRB in liquid medium can also cause precipitation of nano-ZnS with crystalline defects.⁴⁷ The
355 mechanism of SRB influence on nano-ZnS precipitation is not known and might be specific to
356 SRB or an indirect mechanism. Indeed, organic compounds found in bacterial medium or
357 synthesized by bacteria also influence the size of ZnS-particles. For example, simple organic
358 compounds (cysteine and histidine) have been shown to limit ZnS particle growth.^{52,53} Thus,
359 nano-ZnS precipitation in OW is consistent with these previous in-situ observations and bench-
360 scale experiments with SRB and organic compounds.

361 The drastic change in Zn speciation from a majority of nano-ZnS in raw OWs and digestates to
362 a majority of Am-Zn-phosphate in some solid digestates and in all the composts (Figure 2, Table
363 S1) reveals the low stability of nano-ZnS. Some authors already demonstrated that ZnS formed
364 in OW are much less stable after full-scale or bench-scale composting.²²⁻²⁴ This behavior is
365 unexpected compared to what is observed with macroscopic ZnS (i.e. sphalerite). Indeed,
366 sphalerite has been shown to remain stable in the soil for years. Only 0.5% of spiked natural
367 sphalerite had dissolved after one year of incubation in the soil.⁵⁴ Voegelin et al.⁵⁵ observed 26 to
368 97% of dissolution of commercial 25-40 nm (crystallite size) ZnS spiked in four different soils
369 after four years.

370 The low stability of nano-ZnS particles in OWs is probably explained by their small size.
371 Indeed, nanoparticles have a higher proportion of atoms at the surface, making them more
372 reactive and prone to oxidative dissolution. Moreover, for a size of 3.4 nm, Gilbert et al. showed
373 that nano-ZnS present structural disorder⁵⁶ which can increase surface reactivity⁵⁷ and enhance
374 oxidative dissolution. Since ZnS were identified as particles with an average crystallite diameter
375 of about 3 nm in OWs in this study, we assume that the nano-sized ZnS formed in OW explain
376 their instability as soon as they are exposed to aerobic conditions.

377 **Environmental implications**

378 Since Zn speciation determines its availability in amended soil,³⁵ it is crucial to assess Zn
379 speciation in OWs before spreading in order to better predict the fate of Zn in soil. OWs are
380 spread on cultivated soil as fertilizer in raw, digested and/or composted form. Our study
381 evidences the impact of treatment on Zn speciation. Nano-ZnS is the main phase in OWs
382 characterized by reducing conditions (digestates, liquid OWs, liquid digestates, fresh solid
383 digestates). Very few studies have assessed the fate of this species in the soil after OW
384 spreading. Formentini et al.²¹ showed that after spreading of pig slurry, in which nano-ZnS
385 accounted for 100% of the Zn speciation, on a clay soil, all the Zn accumulated in the top 30 cm
386 and was distributed between Zn-OM (41%), Zn-kaolinite (38%) and Zn-FeOx (23%). Zn applied
387 to the soil via pig slurry spreading was no longer present in the form of nano-ZnS. Isaure et al.⁵⁸
388 found that Zn originating from the dissolution of ZnS formed in a sediment was mostly present
389 as Zn sorbed to ferrihydrite in a calcareous and silty soil 18 months after deposition of the
390 sediment on the soil. Thus, soil characteristics appear to influence the fate of Zn after dissolution
391 of nano-ZnS, as shown by Voegelin et al.⁵⁵

392 Amorphous Zn-phosphate is the main phase in samples that have been exposed to oxygen due
393 to their high DM content and storage conditions (solid OWs, composted digestates and OWs,
394 stockpiled solid digestates) followed by Zn sorbed to ferrihydrite. To our knowledge, no results
395 are available about the fate of amorphous zinc phosphate in soil since this phase has not
396 previously been evidenced. Regarding Zn sorbed to ferrihydrite, Tella et al.³⁵ showed that Zn
397 availability increases in OWs-amended clay soil. Zn speciation in these OWs was dominated by
398 Zn sorbed to ferrihydrite and Zn desorption from Fe oxides has been suggested as the mechanism
399 behind the release of Zn in soil solution. Unfortunately, such studies are still scarce and do not
400 cover all the characteristics/properties of the soils that can interact with the fate of TEs.
401 However, the present study provides general trends about the influence of treatments on Zn
402 speciation that could be used for decision-making to limit the environmental impact of
403 agricultural recycling.

404 **Associated content**

405 **Supporting Information.** Results on the influence of sample handling on Zn K-edge EXAFS
406 spectrum; Characterization of reference compounds used for linear combination fitting of Zn K-
407 edge EXAFS spectra; Detailed results of Zn K-edge extended X-ray absorption fine-structure
408 spectroscopy linear combination fitting.

409 **Author information**

410 **Corresponding Author.** Maureen Le Bars * maureenlebars@gmail.com

411 **Acknowledgements**

412 The authors wish to thank J.P. Delgenes, D. Patureau, N. Sertillanges, S. Houot, D.
413 Montenach, A. Savoie (INRA), M. Montès, C. Chevassut-Rosset (CIRAD) who provided us with
414 the samples and considerable advice on sample selection. The authors are grateful to French
415 Environment and Energy Management Agency (ADEME) and the French Agricultural Research
416 Centre for International Development (CIRAD) for funding the PhD scholarship of Maureen Le
417 Bars. This study was part of the DIGESTATE project, funded by ANR (*Agence Nationale de la*
418 *Recherche*, France) under Grant ANR-15-CE34-0003-01. We acknowledge the European
419 Synchrotron Radiation Facility (ESRF) and Stanford Synchrotron Radiation Light- source
420 (SSRL) for provision of synchrotron radiation facilities. Use of the SSRL, SLAC National
421 Accelerator Laboratory, was supported by the U.S. Department of Energy, Office of Science,
422 Office of Basic Energy Sciences under Contract No. DE-AC02- 76SF00515. The authors declare
423 no competing financial interest.

424 **References**

- 425 1. Hoornweg, D., Bhada-Tata P., Kennedy, C. Waste production must peak this century.
426 *Nature* **2013**, *502* (7473), 615-617.
- 427 2. Gomez, C. D. C. Biogas as an energy option: an overview. In *The Biogas Handbook:*
428 *Science, Production and Applications*, Wellinger, A., Murphy, J., Baxter, D., Ed. Woodhead
429 Publishing Limited: Cambridge 2013; pp 1-15.
- 430 3. Al Seadi, T.; Drog, B.; Fuchs, W.; Rutz, D.; Janssen, R. Biogas digestate quality and
431 utilization. In *The Biogas Handbook – Science, Production and Applications*, , Wellinger, A.,
432 Murphy, J., Baxter, D., Ed. Woodhead Publishing Limited: Cambridge 2013; pp 267-301.
- 433 4. Möller, K.; Müller, T. Effects of anaerobic digestion on digestate nutrient availability and
434 crop growth: A review. *Eng. Life Sci.* **2012**, *12* (3), 242-257.
- 435 5. Nkoa, R. Agricultural benefits and environmental risks of soil fertilization with anaerobic
436 digestates: a review. *Agron. Sustain. Dev.* **2014**, *34* (2), 473-492.
- 437 6. Belon, E.; Boisson, M.; Deportes, I.; Eglin, T.; Feix, I.; Bispo, A.; Galsomies, L.;
438 Leblond, S.; Guellier, C. An inventory of trace elements inputs to French agricultural soils. *Sci.*
439 *Total Environ.* **2012**, *439*, 87-95.

- 440 7. Leclerc, A.; Laurent, A. Framework for estimating toxic releases from the application of
441 manure on agricultural soil: National release inventories for heavy metals in 2000-2014. *Sci.*
442 *Total Environ.* **2017**, *590*, 452-460.
- 443 8. Alburquerque, J. A.; de la Fuente, C.; Ferrer-Costa, A.; Carrasco, L.; Cegarra, J.; Abad,
444 M.; Bernal, M. P. Assessment of the fertiliser potential of digestates from farm and
445 agroindustrial residues. *Biomass Bioenerg.* **2012**, *40*, 181-189.
- 446 9. Tampio, E.; Salo, T.; Rintala, J. Agronomic characteristics of five different urban waste
447 digestates. *J. Environ. Manage.* **2016**, *169*, 293-302.
- 448 10. Pathak, A.; Dastidar, M. G.; Sreekrishnan, T. R. Bioleaching of heavy metals from
449 sewage sludge: a review. *J. Environ. Manage.* **2009**, *90* (8), 2343-53.
- 450 11. Smith, S. R. A critical review of the bioavailability and impacts of heavy metals in
451 municipal solid waste composts compared to sewage sludge. *Environ. Int.* **2009**, *35* (1), 142-56.
- 452 12. Jin, X. F.; Yang, X. E.; Islam, E.; Liu, D.; Mahmood, Q.; Li, H.; Li, J. Ultrastructural
453 changes, zinc hyperaccumulation and its relation with antioxidants in two ecotypes of *Sedum*
454 *alfredii* Hance. *Plant Physiol. Bioch.* **2008**, *46* (11), 997-1006.
- 455 13. Alonso-Blázquez, N.; García-Gómez, C.; Fernández, M. D. Influence of Zn-contaminated
456 soils in the antioxidative defence system of wheat (*Triticum aestivum*) and maize (*Zea mays*) at
457 different exposure times: potential use as biomarkers. *Ecotoxicology* **2015**, *24* (2), 279-291.
- 458 14. Chaudri, A. M.; Allain, C. M. G.; Barbosa-Jefferson, V. L.; Nicholson, F. A.; Chambers,
459 B. J.; McGrath, S. P. A study of the impacts of Zn and Cu on two rhizobial species in soils of a
460 long-term field experiment. *Plant Soil* **2000**, *221* (2), 167-179.
- 461 15. Wang, C.; Zhang, S. H.; Wang, P. F.; Hou, J.; Zhang, W. J.; Li, W.; Lin, Z. P. The effect
462 of excess Zn on mineral nutrition and antioxidative response in rapeseed seedlings. *Chemosphere*
463 **2009**, *75* (11), 1468-1476.
- 464 16. Collin, B.; Doelsch, E. Impact of high natural soilborne heavy metal concentrations on
465 the mobility and phytoavailability of these elements for sugarcane. *Geoderma* **2010**, *159* (3-4),
466 452-458.
- 467 17. Saveyn, H.; Eder, P.; Garbarino, E.; Muchova, L.; Hjelmar, O.; van der Sloot, H.;
468 Comans, R.; van Zomeren, A.; Hyks, J.; Oberender, A. *Study on methodological aspects*
469 *regarding limit values for pollutants in aggregates in the context of the possible development of*
470 *end-of-waste criteria under the EU Waste Framework Directive*; Publications Office of the
471 European Union: Luxembourg, 2014.
- 472 18. Nolan, A. L.; Lombi, E.; McLaughlin, M. J. Metal bioaccumulation and toxicity in
473 soils—why bother with speciation? *Aust. J. Chem.* **2003**, *56* (3), 77-91.
- 474 19. Gelabert, A.; Sivry, Y.; Gobbi, P.; Mansouri-Guilani, N.; Menguy, N.; Brayner, R.; Siron,
475 V.; Benedetti, M. F.; Ferrari, R. Testing nanoeffect onto model bacteria: Impact of speciation and
476 genotypes. *Nanotoxicology* **2016**, *10* (2), 216-225.
- 477 20. Legros, S.; Levard, C.; Marcato-Romain, C. E.; Guiresse, M.; Doelsch, E. Anaerobic
478 Digestion Alters Copper and Zinc Speciation. *Environ. Sci. Technol.* **2017**, *51* (18), 10326-
479 10334.
- 480 21. Formentini, T. A.; Legros, S.; Fernandes, C. V. S.; Pinheiro, A.; Le Bars, M.; Levard, C.;
481 Mallmann, F. J. K.; Da Veiga, M.; Doelsch, E. Radical change of Zn speciation in pig slurry
482 amended soil: Key role of nano-sized sulfide particles. *Environ. Pollut.* **2017**, *222*, 495-503.
- 483 22. Nagoshi, M.; Kawano, T.; Fujiwara, S.; Miura, T.; Udagawa, S.; Nakahara, K.; Takaoka,
484 M.; Uruga, T. Chemical states of trace heavy metals in sewage sludge by XAFS spectroscopy.
485 *Phys. Scripta* **2005**, *2005* (T115), 946.

- 486 23. Donner, E.; Howard, D. L.; Jonge, M. D. d.; Paterson, D.; Cheah, M. H.; Naidu, R.;
487 Lombi, E. X-ray Absorption and Micro X-ray Fluorescence Spectroscopy Investigation of
488 Copper and Zinc Speciation in Biosolids. *Environ. Sci. Technol.* **2011**, *45* (17), 7249-7257.
- 489 24. Lombi, E.; Donner, E.; Tavakkoli, E.; Turney, T. W.; Naidu, R.; Miller, B. W.; Scheckel,
490 K. G. Fate of Zinc Oxide Nanoparticles during Anaerobic Digestion of Wastewater and Post-
491 Treatment Processing of Sewage Sludge. *Environ. Sci. Technol.* **2012**, *46* (16), 9089-9096.
- 492 25. Donner, E.; Brunetti, G.; Zarcinas, B.; Harris, P.; Tavakkoli, E.; Naidu, R.; Lombi, E.
493 Effects of Chemical Amendments on the Lability and Speciation of Metals in Anaerobically
494 Digested Biosolids. *Environ. Sci. Technol.* **2013**, *47* (19), 11157-11165.
- 495 26. Kim, B.; Levard, C.; Murayama, M.; Brown, G. E.; Hochella, M. F. Integrated
496 Approaches of X-Ray Absorption Spectroscopic and Electron Microscopic Techniques on Zinc
497 Speciation and Characterization in a Final Sewage Sludge Product. *J. Environ. Qual.* **2014**, *43*
498 (3), 908-916.
- 499 27. Legros, S.; Doelsch, E.; Masion, A.; Rose, J.; Borshneck, D.; Proux, O.; Hazemann, J. L.;
500 Saint-Macary, H.; Bottero, J. Y. Combining Size Fractionation, Scanning Electron Microscopy,
501 and X-ray Absorption Spectroscopy to Probe Zinc Speciation in Pig Slurry. *J. Environ. Qual.*
502 **2010**, *39* (2), 531-540.
- 503 28. Legros, S.; Chaurand, P.; Rose, J. r.; Masion, A.; Briois, V.; Ferrasse, J.-H.; Macary, H.
504 S.; Bottero, J.-Y.; Doelsch, E. Investigation of copper speciation in pig slurry by a
505 multitechnique approach. *Environ. Sci. Technol.* **2010**, *44* (18), 6926-6932.
- 506 29. Auffan, M.; Rose, J.; Bottero, J.-Y.; Lowry, G. V.; Jolivet, J.-P.; Wiesner, M. R. Towards
507 a definition of inorganic nanoparticles from an environmental, health and safety perspective. *Nat.*
508 *Nanotechnol.* **2009**, *4* (10), 634-641.
- 509 30. Khalid, A.; Arshad, M.; Anjum, M.; Mahmood, T.; Dawson, L. The anaerobic digestion
510 of solid organic waste. *Waste Manage.* **2011**, *31* (8), 1737-1744.
- 511 31. Birks, L. S.; Friedman, H. Particle Size Determination from X-Ray Line Broadening. *J.*
512 *Appl. Phys.* **1946**, *17* (8), 687-692.
- 513 32. Bach, S.; Celinski, V. R.; Dietzsch, M.; Panthofer, M.; Bienert, R.; Emmerling, F.;
514 Schmedt auf der Gunne, J.; Tremel, W. Thermally highly stable amorphous zinc phosphate
515 intermediates during the formation of zinc phosphate hydrate. *J. Am. Chem. Soc.* **2015**, *137* (6),
516 2285-94.
- 517 33. Doelsch, E.; Basile-Doelsch, I.; Rose, J.; Masion, A.; Borschneck, D.; Hazemann, J.-L.;
518 Saint Macary, H.; Bottero, J.-Y. New combination of EXAFS spectroscopy and density
519 fractionation for the speciation of chromium within an andosol. *Environ. Sci. Technol.* **2006**, *40*
520 (24), 7602-7608.
- 521 34. Ravel, B.; Newville, M. ATHENA, ARTEMIS, HEPHAESTUS: data analysis for X-ray
522 absorption spectroscopy using IFEFFIT. *J. Synchrotron Radiat.* **2005**, *12* (4), 537-541.
- 523 35. Tella, M.; Bravin, M. N.; Thuriès, L.; Cazevieuille, P.; Chevassus-Rosset, C.; Collin, B.;
524 Chaurand, P.; Legros, S.; Doelsch, E. Increased zinc and copper availability in organic waste
525 amended soil potentially involving distinct release mechanisms. *Environ. Pollut.* **2016**, *212*, 299-
526 306.
- 527 36. Hammer, D.; Keller, C.; McLaughlin, M. J.; Hamon, R. E. Fixation of metals in soil
528 constituents and potential remobilization by hyperaccumulating and non-hyperaccumulating
529 plants: Results from an isotopic dilution study. *Environ. Pollut.* **2006**, *143* (3), 407-415.

530 37. Pokrovsky, O. S.; Pokrovski, G. S.; Gélabert, A.; Schott, J.; Boudou, A. Speciation of Zn
531 associated with diatoms using X-ray absorption spectroscopy. *Environ. Sci. Technol.* **2005**, *39*
532 (12), 4490-4498.

533 38. Rose, J.; Moulin, I.; Masion, A.; Bertsch, P. M.; Wiesner, M. R.; Bottero, J.-Y.; Mosnier,
534 F.; Haehnel, C. X-ray absorption spectroscopy study of immobilization processes for heavy
535 metals in calcium silicate hydrates. 2. Zinc. *Langmuir* **2001**, *17* (12), 3658-3665.

536 39. Sammut, M.; Rose, J.; Masion, A.; Fiani, E.; Depoux, M.; Ziebel, A.; Hazemann, J.;
537 Proux, O.; Borschneck, D.; Noack, Y. Determination of zinc speciation in basic oxygen furnace
538 flying dust by chemical extractions and X-ray spectroscopy. *Chemosphere* **2008**, *70* (11), 1945-
539 1951.

540 40. Zirkler, D.; Peters, A.; Kaupenjohann, M. Elemental composition of biogas residues:
541 Variability and alteration during anaerobic digestion. *Biomass Bioenerg.* **2014**, *67*, 89-98.

542 41. Tambone, F.; Genevini, P.; D'Imporzano, G.; Adani, F. Assessing amendment properties
543 of digestate by studying the organic matter composition and the degree of biological stability
544 during the anaerobic digestion of the organic fraction of MSW. *Bioresource Technol.* **2009**, *100*
545 (12), 3140-2.

546 42. Knoop, C.; Tietze, M.; Dornack, C.; Raab, T. Fate of nutrients and heavy metals during
547 two-stage digestion and aerobic post-treatment of municipal organic waste. *Bioresource Technol.*
548 **2017**, *251*, 238-248.

549 43. Knoop, C.; Dornack, C.; Raab, T. Nutrient and heavy metal accumulation in municipal
550 organic waste from separate collection during anaerobic digestion in a two-stage laboratory
551 biogas plant. *Bioresource Technol.* **2017**, *239*, 437-446.

552 44. Nicholson, F.; Chambers, B.; Williams, J.; Unwin, R. Heavy metal contents of livestock
553 feeds and animal manures in England and Wales. *Bioresource Technol.* **1999**, *70* (1), 23-31.

554 45. Romeo, A.; Vacchina, V.; Legros, S.; Doelsch, E. Zinc fate in animal husbandry systems.
555 *Metallomics* **2014**, *6* (11), 1999-2009.

556 46. Moreau, J. W.; Webb, R. I.; Banfield, J. F. Ultrastructure, aggregation-state, and crystal
557 growth of biogenic nanocrystalline sphalerite and wurtzite. *Am. Mineral.* **2004**, *89* (7), 950-690.

558 47. Xu, J.; Murayama, M.; Roco, C. M.; Veeramani, H.; Marc Michel, F.; Donald Rimstidt,
559 J.; Winkler, C.; Hochella Jr, M. F. Highly-Defective Nanocrystals of ZnS Formed via
560 Dissimilatory Bacterial Sulfate Reduction: a Comparative Study with their Abiogenic
561 Analogues. *Geochim. Cosmochim. Acta* **2016**, *180*, 1-14.

562 48. Peltier, E.; Ilipilla, P.; Fowle, D. Structure and reactivity of zinc sulfide precipitates
563 formed in the presence of sulfate-reducing bacteria. *Appl. Geochem.* **2011**, *26* (9-10), 1673-
564 1680.

565 49. Brehler B.; Wedepohl, K. H. Zinc. In *Handbook of Geochemistry*, Wedepohl, K., Ed.
566 Springer-Verlag: Berlin 1978; Vol. II/3.

567 50. Chen, Y.; Cheng, J. J.; Creamer, K. S. Inhibition of anaerobic digestion process: a review.
568 *Bioresource Technol.* **2008**, *99* (10), 4044-64.

569 51. Moreau, J. W.; Weber, P. K.; Martin, M. C.; Gilbert, B.; Hutcheon, I. D.; Banfield, J. F.
570 Extracellular Proteins Limit the Dispersal of Biogenic Nanoparticles. *Science* **2007**, *316* (5831),
571 1600-1603.

572 52. Gondikas, A. P.; Masion, A.; Auffan, M.; Lau, B. L. T.; Hsu-Kim, H. Early-stage
573 precipitation kinetics of zinc sulfide nanoclusters forming in the presence of cysteine. *Chem.*
574 *Geol.* **2012**, *329*, 10-17.

- 575 53. Kaur, J.; Sharma, M.; Pandey, O. P. Effect of pH on Size of ZnS Nanoparticles and Its
576 Application for Dye Degradation. *Particul. Sci. Technol.* **2015**, *33* (2), 184-188.
- 577 54. Robson, T. C.; Braungardt, C. B.; Rieuwerts, J.; Worsfold, P. Cadmium contamination of
578 agricultural soils and crops resulting from sphalerite weathering. *Environ. Pollut.* **2014**, *184*,
579 283-289.
- 580 55. Voegelin, A.; Jacquat, O.; Pfister, S.; Barmettler, K.; Scheinost, A. C.; Kretzschmar, R.
581 Time-Dependent Changes of Zinc Speciation in Four Soils Contaminated with Zincite or
582 Sphalerite. *Environ. Sci. Technol.* **2011**, *45* (1), 255-261.
- 583 56. Gilbert, B.; Huang, F.; Zhang, H.; Waychunas, G. A.; Banfield, J. F. Nanoparticles:
584 Strained and Stiff. *Science* **2004**, *305* (5684), 651-654.
- 585 57. Waychunas, G. A.; Zhang, H. Structure, Chemistry, and Properties of Mineral
586 Nanoparticles. *Elements* **2008**, *4* (6), 381-387.
- 587 58. Isaure, M.-P.; Manceau, A.; Geoffroy, N.; Laboudigue, A.; Tamura, N.; Marcus, M. A.
588 Zinc mobility and speciation in soil covered by contaminated dredged sediment using
589 micrometer-scale and bulk-averaging X-ray fluorescence, absorption and diffraction techniques.
590 *Geochim. Cosmochim. Acta* **2005**, *69* (5), 1173-1198.

591

592